Effects of Experimental Diabetes on the Structure and Ultrastructure of the Coagulating Gland of C57BL/6J and NOD Mice

C.A.F. CARVALHO,[1] A.M. CAMARGO,[3] V.H.A. CAGNON,[1]* AND C.R. PADOVANI[2]

[1]Department of Anatomy, Institute of Biology, State University of Campinas, Campinas-SP, Brazil

[2]Department of Anatomy, Institute of Bioscience, State University of São Paulo, Botucatu-SP, Brazil

[3]Department of Anatomy, University of South Santa Catarina, Santa Catarina, Brazil

ABSTRACT

Diabetes mellitus can lead to reproductive disorders that in turn result in weakened fertility brought about by morphofunctional changes in the testes and accessory sex glands. However, doubts persist concerning the basic biology of the secretory epithelial cells and the stroma of the coagulating gland of diabetic mice. Thus, the objective of the present study was to analyze the histological and ultrastructural changes associated with stereology of the coagulating gland of mice with alloxan-induced diabetes, and of spontaneously diabetic mice. Sixteen mice of the C57BL/6J strain, and eight non-obese diabetic (NOD) mice were used. The animals were divided into three groups: 1) control (C), 2) alloxan diabetic (AD), and 3) NOD. Thirty days after the detection of diabetic status in group 2, all of the animals were killed and then perfused with Karnovsky's solution through the left cardiac ventricle. The coagulating gland was then removed and processed for morphometric study by light microscopy and electron microscopy. The results showed thickening of the stroma, atrophy of secretory epithelial cells, and disorganization of the organelles involved in the secretory process in both NOD and alloxan-induced mice. Thus, it may be concluded that the coagulating gland suffered drastic morphological changes, and consequently impaired glandular function, in the presence of diabetes mellitus type I in both NOD and AD mice. Anat Rec Part A 270A:129–136, 2003.

Key words: coagulating gland; histology; ultrastructure; stereology; non-obese diabetic (NOD); alloxan

The coagulating gland is present in guinea pigs, rats, hamsters, mice, and monkeys (Sjöstrand, 1965). This gland is also known as the anterior prostate or dorsocranial lobe because of its embryonic development from the urogenital sinus and the prostatic complex (Narbaitz, 1974; Cavazos, 1975). According to Price (1963), embryologically there is homology between this gland and the middle prostatic lobe in men. In rodents, the coagulating gland is located in the concavity of the seminal vesicle, and produces secretions rich in fructose and proteins, as dorsal I, II, vesiculase and transglutaminase involved in semen coagulation and sperm motility (Cavazos, 1975; Wilson and French, 1980; Aumüller and Seitz, 1990; Cukierski et al., 1991) and in the formation of the copulatory plug in females (Bradshaw and Wolfe, 1977; Carballada

Grant sponsor: CAPES.

*Correspondence to: Dr. Valeria H.A. Cagnon, Departamento de Anatomia, Instituto de Biologia, Universidade Estadual de Campinas (UNICAMP) 13084-971, Campinas, São Paulo, Brasil. Fax: +55-19-3289-3124. E-mail: quitete@uol.com.br

Received 15 May 2002; Accepted 1 October 2002

DOI 10.1002/ar.a.10014

and Esponda, 1992). Like the prostatic lobes and the seminal vesicle, the coagulating gland is androgen-dependent. The depletion or absence of androgens in serum, as occurs with the use of an anti-androgen agent or after castration, promotes the rapid involution of these accessory sex organs, accompanied by morphofunctional changes (Rennie et al., 1984). In addition to castration, conditions such as alcoholism (Cagnon et al., 1996, 2000), cigarette smoking (Reddy et al., 1998), and diabetes (Daubresse et al., 1978) are known to alter circulating levels of testosterone and consequently the functioning of accessory sex glands. Among these diseases, childhood diabetes and insulin-dependent diabetes mellitus (IDDM) (characterized by a severe or complete lack of insulin, and a tendency to develop ketosis (Stefan, 1996)) are particularly important. It is known that diabetes affects different organ systems, such as the urinary and circulatory systems, as well as the nervous system (Stefan, 1996). Type 1, or IDDM, occurs in approximately 10% of all diabetic patients in the Western world (Stefan, 1996). The occurrence of IDDM during adolescence may impair the development of accessory sex organs associated with hormonal activity (Stefan, 1996). Some studies have suggested that diabetes is correlated with sexual impotence and infertility (Daubresse et al., 1978), as well as with cancer of the prostate (Will et al., 1999). Atrophy of the secretory epithelium of the ventral prostate has also been experimentally demonstrated in rodents considered to be diabetic (Cagnon et al., 2000). Despite the known harmful effects of diabetes on the secretory epithelium of accessory sex glands, doubts persist about the stroma–epithelium interaction, which is an important factor in the diagnosis of diseases that frequently involve these glands, and there is a lack of detailed information about the involvement of organelles participating in the glandular secretory process.

On this basis, the objective of the present study was to assess histologic and ultrastructural factors associated with stereology of the coagulating gland of mice with type I diabetes.

MATERIALS AND METHODS

Animals and Tissue Preparation

A total of 24 adult male mice (16 C57BL/6J mice and eight non-obese diabetic (NOD) mice, all 4 months old) were divided into three groups of eight animals each: control (C), alloxan diabetic (AD), and spontaneously diabetic (NOD). The AD group received alloxan as the diabetogenic agent (Sigma Chemical Company, St. Louis, MO) administered in 0.1 M citrate buffer (pH 4.4) as vehicle. Each animal received five intraperitoneal injections at 7-day intervals. The first three doses were 75 mg/kg body weight, and the two remaining doses were 150 mg/kg per animal. The C and NOD groups simultaneously received 0.1 ml 0.1 M citrate buffer (pH 4.4) intraperitoneally. All animals received balanced granulated solid Nuvilab (Nuvital®, Colombo, PR, Brazil) chow ad libitum. The diabetic status of the animals was characterized using Multistix 10-SG reagents strips (Bayer®, San Andrés, Buenos Aires, Argentina) to determine the approximate variation of glucose (mg/dl) in urine. Two Multistix 10-SG tests were performed each animal before the first alloxan injection for quantitative analysis of glucose as a control standard. Thirty days after the characterization of diabetic status, the animals of the three experimental groups were anesthetized with Francotar and Virbaxil (Vibrac®, Roseira, SP, Brazil), 1/1 0.25 ml/0.1 kg, and then killed. The coagulating glands were then removed from four mice in each group and fixed in Bouin's fluid. Tissue samples were embedded in Paraplast Plus (Paraplast®, St. Louis, MO) processed for routine light microscopy, and stained with hematoxylin and eosin (H&E). The four remaining mice in each group were perfused (Sprando, 1990) with heparinized physiological saline followed by Karnovsky's fixing solution (Karnovsky, 1965). Samples of the coagulating gland were immediately removed and fixed in 3% glutaraldehyde and 1% paraformaldehyde in 0.1 M phosphate buffer (pH 7.4) for a period of 3 hr, and postfixed in 1% osmium tetroxide in the same buffer for 2 hr. The material was then dehydrated in a growing acetone series and embedded in plastic resin (Polyscience®, Niles, IL). Sections of 0.5 μm were stained with toluidine blue and prepared for light microscopy for the selection of specific areas to be examined by transmission electron microscopy (TEM). Ultrathin sections were obtained with an LKB ultramicrotome and contrasted with uranyl acetate (Watson, 1958) and lead citrate (Reynolds, 1963). Electron micrographs were obtained with an LEO 906 electron microscope.

Morphometric Procedures

The cellular, cytoplasmic, and nuclear volumes were measured on the sections stained for light microscopy. Cytoplasm and nuclear volumes were measured without knowledge of the treatment being administered at ×100 magnification using the point-counting method described by Weibel (1979). Data for nuclear volume were recorded as the average obtained with 50 measurements per experimental group. Long and short axes were measured, and the mean nuclear volume was calculated considering nuclei as ellipsoids. The Image-pro® Express Version 4 software with a 10× objective was used to determine % relative area (stroma × glandular mucosa) ,and the density of the digestive and secretory vacuole areas was determined using current stereology methods and formulae as described by Weibel et al. (1966). A multipurpose test system with 84 lines and 168 points was applied to 15 electron micrographs (×10,000) per group, and the numerical density of the area was estimated.

Statistical Analysis

The nonparametric Kruskal-Wallis test was used to analyze data concerning cytoplasmic nuclear volume (μm^3) and nuclear shape, complemented with the multiple-comparisons test of Student-Newman-Keuls, with the level of significance set at 5% in all analyses (Wichern and Johnson, 1992).

RESULTS

Urine Analysis

The control animals had an average urinary glucose level of 0 mg/dl in 100% of the samples. The animals from the diabetic groups had an average urinary glucose level of 1,250 mg/dl.

Light Microscopy

The coagulating glands of the control mice presented stroma containing smooth muscle, collagen fibers, and blood vessels, arranged around the acini (Fig. 1A). The

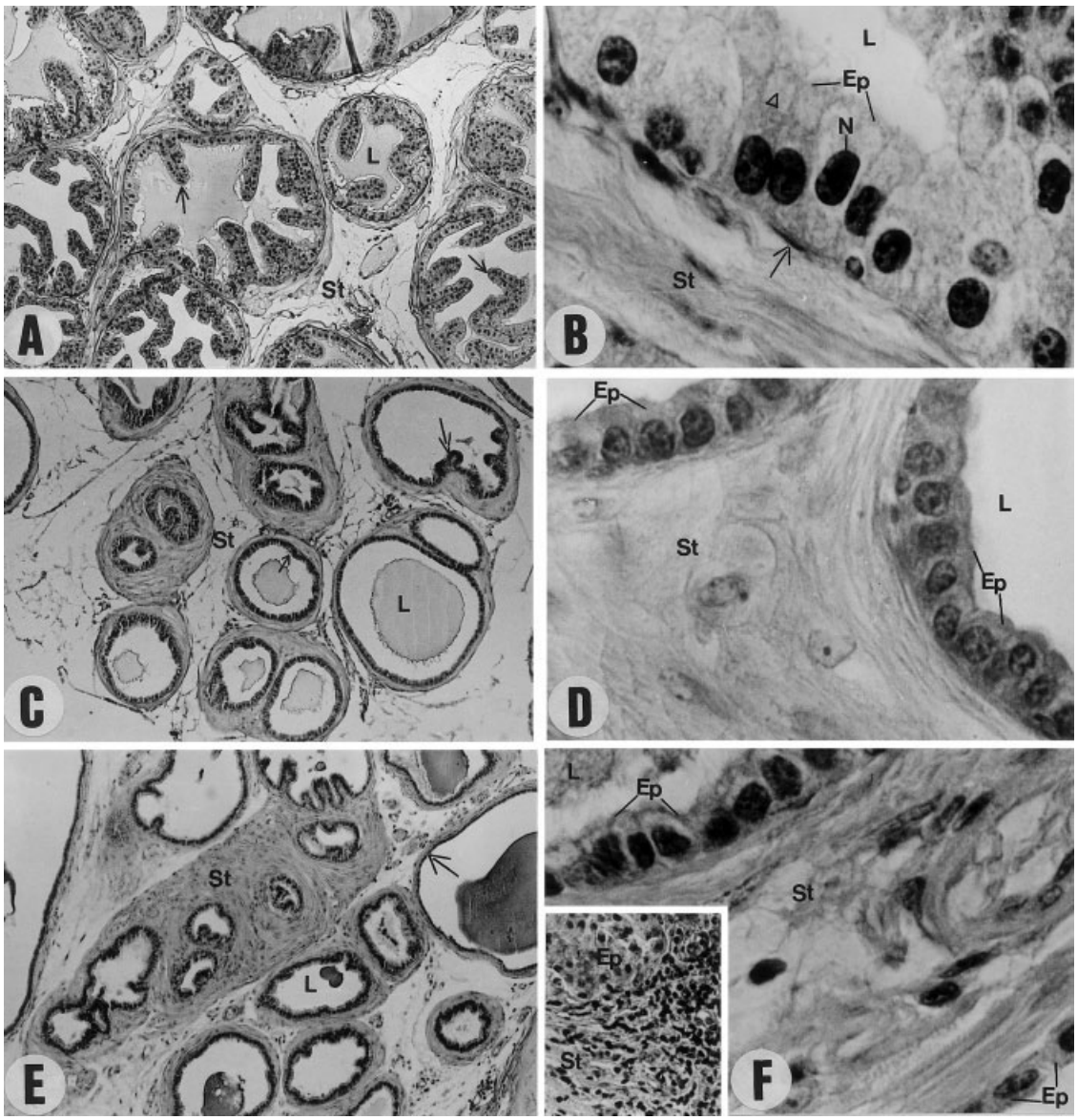

Fig. 1. Photomicrographs of the coagulating glands of control and diabetic mice. **A:** Control group. St, stroma. Acini with infolded glandular mucosa (arrow). L, lumen. ×253 H&E. **B:** Control group. Epithelial cells (Ep) of the tall columnar type with centrally located nuclei (N). Light zones in the supranuclear region (arrowhead). Underlying the epithelial cells, stroma containing smooth muscle cells intermingled with collagen fibers. Lumen containing secretions of homogeneous aspect (L) ×1,253 H&E. **C** and **E:** Diabetic groups. Intensely thickened stroma. Acini with slightly infolded glandular mucosa (arrow). ×253 H&E. **D** and **F:** Diabetic groups. Epithelial cells (Ep) with marked cytoplasmic and nuclear atrophy (Ep). In the stroma (St), observe the apparently hypertrophied smooth muscle cells. Lumen containing secretion of floccular aspect (L). ×1,253 H&E. Inset: Detail of the glandular stroma with an inflammatory infiltrate in NOD animals. C and D: AD animals. E and F: NOD animal.

glandular mucosa was infolded (Fig. 1A), with a simple secretory epithelium and tall columnar cells. Eventual basal cells were intermingled with columnar cells. The cell nuclei were elliptical in shape and occupied a central position (Fig. 1B; Table 1). AD and NOD mice showed thickening of the stroma (Figs. 1A and 2A) and spacing between acini, in addition to a slightly infolded glandular mucosa (Fig. 1C and E). Inflammatory infiltrate was observed in the stromal region, especially in NOD animals (Fig. 1F, inset). The cells of the secretory epithelium showed significant atrophy of the cytoplasmic volume and alteration of the nuclear shape, which had become spherical. Nuclear volume was also reduced, but not significantly so (Fig. 1D and F; Table 1).

TEM

Ultrastructurally, the control group showed tall, columnar epithelial cells resting on a clearly visible and intact basal lamina. Underlying the basal lamina were smooth muscle cells, collagen, and elastic fibers. The nucleus was elliptical in shape, containing condensed chromatin in the peripheral region (Fig. 3A). In the basal region of the cells

TABLE 1. Nuclear volume, nuclear shape and cytoplasmic volume of the coagulating gland of animals from the control, alloxan diabetic (Alloxan D) and spontaneously diabetic NOD (Spont. NOD D) groups

Group				
Variable	Control	Alloxan D	NOD D	Result of the test
V. nucleus	74.29 ± 17.88[a]	44.45 ± 13.42[a]	42.60 ± 16.44[a]	4.96 ($P>0.05$)
F. nucleus	1.72 ± 0.07[b]	1.05 ± 0.02[a]	1.03 ± 0.01[a]	8.02 ($P<0.05$)
Cytopl. vol.	405.34 ± 163.189[b]	85.50 ± 30.93[a]	82.11 ± 24.73[a]	7.54 ($P<0.05$)

[a,b]Mean comparison between experimental groups.
Data are reported as means ± SEM.

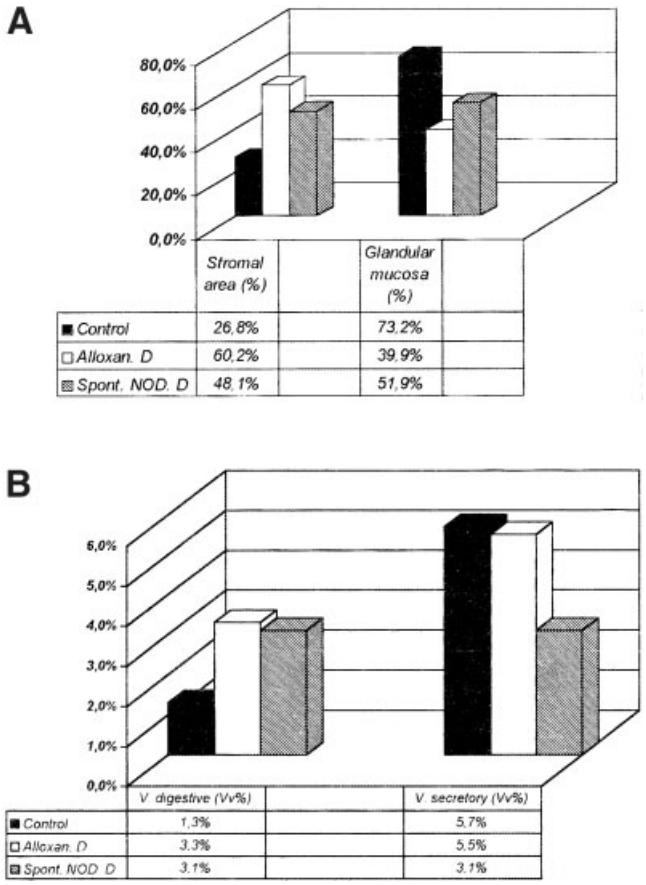

Fig. 2. **A:** The % relative area (stroma × glandular mucosa) of the coagulating glands of C, AD, and NOD animals. **B:** Relative volume (Vv%) of the digestive and secretory vacuoles of the epithelial cells of the coagulating gland of C, AD, and NOD animals.

there were dilated cisterns of the granular endoplasmic reticulum (GER) containing material of low electron density (Fig. 3B). In the supranuclear cytoplasm there was a well-developed Golgi complex surrounding secretory vacuoles in various stages of maturation (Figs. 2B and 3C). There were also occasional digestive vacuoles in the cell cytoplasm (Fig. 2B). Sparse and small microvilli were also observed on the cell surface (Fig. 3D). In animals with spontaneous and alloxan-induced diabetes, the major changes (compared to control mice) were hypertrophy of extracellular matrix components (Figs. 4G (inset) and 3A (inset)) and an accumulation of different polymorphic nuclei, characterizing an inflammatory cellular infiltrate (Fig. 4C). Also, the epithelial cells were markedly atrophied (Fig. 4A); their nuclei occupied a large part of the cytoplasm, and showed an irregular shape (Fig. 4A and B) as well as condensed chromatin (Fig. 4B). The basal cell cytoplasm showed intensified reduced cisterns of the granular endoplasmic reticulum (Fig. 4A and G) and the presence of highly electron-dense digestive vacuoles (Figs. 2B and 4A). The Golgi complex presented dilated cisterns (Fig. 4F) and eventual secretion granules were observed in the apical region (Fig. 2B). Ruptured microvilli on the cell surface facing the lumen were noted secondarily (Fig. 4D and E). An intensified presence of free ribosomes was observed in the cytoplasm of epithelial cells (Fig. 4D and F).

DISCUSSION

In the present study, diabetic status was characterized by high glucose levels in an animal's urine. The occurrence of glycosuria is one of the determining factors in the identification of diabetes type I; it has been demonstrated both in animals submitted to different diabetogenic drugs and in spontaneously diabetic animals (Hunt and Bailey, 1961; Makino et al., 1980; Ader et al., 1998). Thus, it may be concluded that both the mice submitted to chemical induction with alloxan and the mice with spontaneously generated diabetes (NOD) manifested diabetes in an effective manner, confirming the validity of the experimental model.

The present histological results demonstrated important changes in the coagulation gland of both AD and NOD mice. Particularly important among these changes was stromal tissue hypertrophy with the occurrence of an inflammatory cell infiltrate, in addition to intense volumetric atrophy of secretory epithelial cells, with a predominance of the cytoplasmic portion and nuclear deformity in the coagulation gland. Previous studies on the ventral lobe of the prostate of diabetic rats and mice demonstrated atrophy of the secretory epithelial cells and enlargement of the stromal region (Hunt and Bailey, 1961; Jackson and Hutson, 1984; Cagnon et al., 2000). Several experiments carried out to analyze accessory sex glands, including the coagulation gland, under androgen deprivation showed a disorganized morphology of the secretory epithelium and the stroma, with an increase in smooth muscle cells and collagen, and elastic fibers in the ventral lobe of the prostate of castrated rats (Aumüller, 1977; Mariotti et al., 1987; De Carvalho and Line, 1996; Kiess and Gallaher, 1998). These structural characteristics were found to be correlated with maintenance mechanisms for the integrity of the secretory epithelium (De Carvalho and Line, 1996). The stroma–epithelium interaction is known to be of fun-

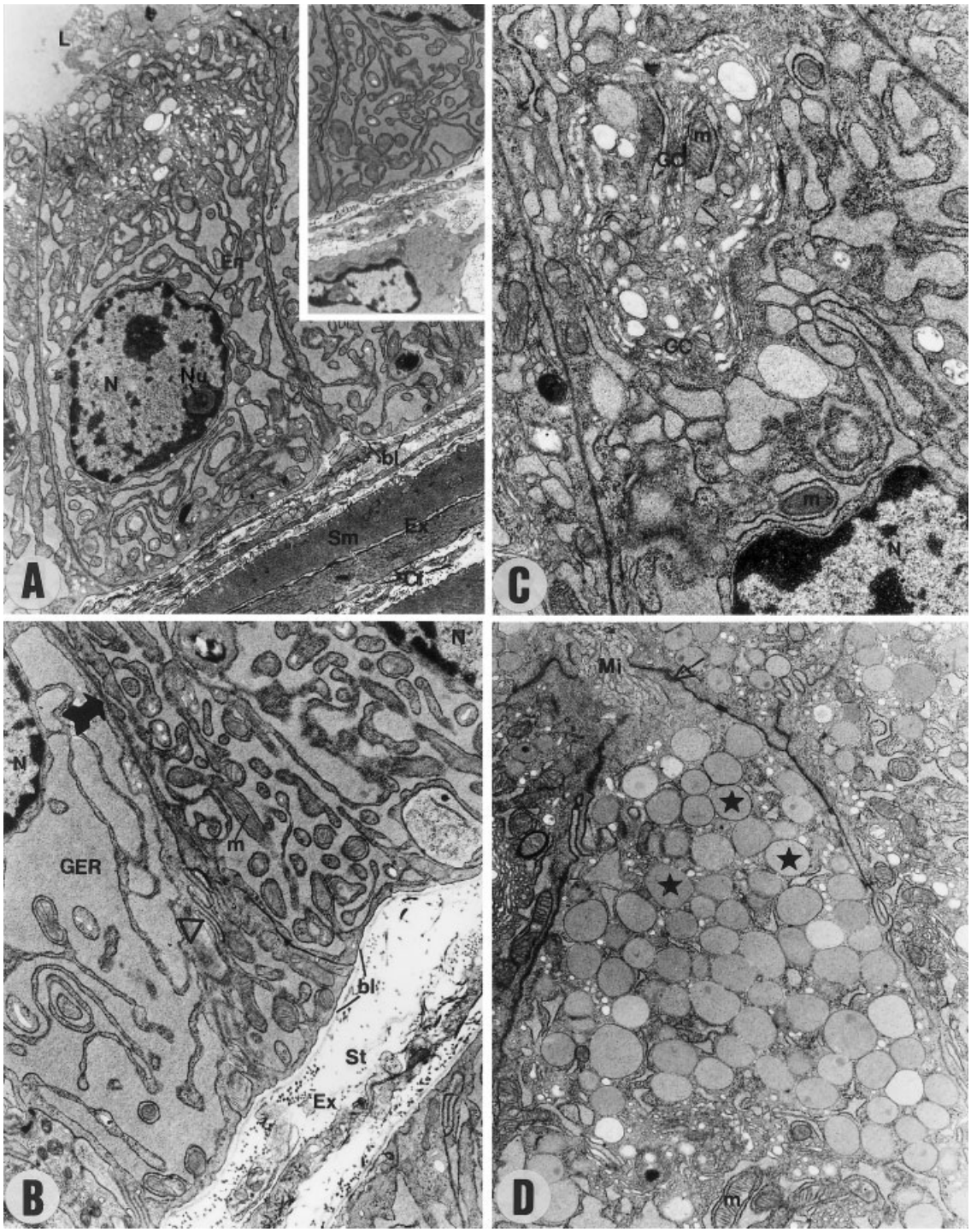

Fig. 3. Electron micrographs of the coagulating glands of control mice. **A:** Simple epithelium with tall columnar cells. Central nucleus (N) with a clearly visible envelope (En) and nucleolus (Nu). Condensed chromatin and the nuclear periphery. Extracellular matrix with smooth muscle cells (Sm) and collagen fibers (Cf). Intact basal lamina (bl). Region of the extracellular matrix (Ex). Lumen (L) ×6,120. Inset: Extracellular matrix detail ×3,672. **B:** Basal region. Dilated cisterns of the granular endoplasmic reticulum (GER). Intact plasmatic membrane (→). Mitochondria with clearly visible cristae (m). Clearly visible basal lamina (bl). Region of the extracellular matrix (Ex). Nucleus (N) ×12,000. **C:** Detail of the supranuclear region. Mitochondria (m) surrounding a well-developed Golgi complex (GC). Nucleus (N) ×18,000. **D:** Apical region: Accumulation of vacuoles containing secretion of floccular aspect and varied electron density (★). Intact intercellular junctions (arrows). Mitochondria with intact cristae (mi). Luminal surface with small microvilli (mi). Lumen (L) ×12,000.

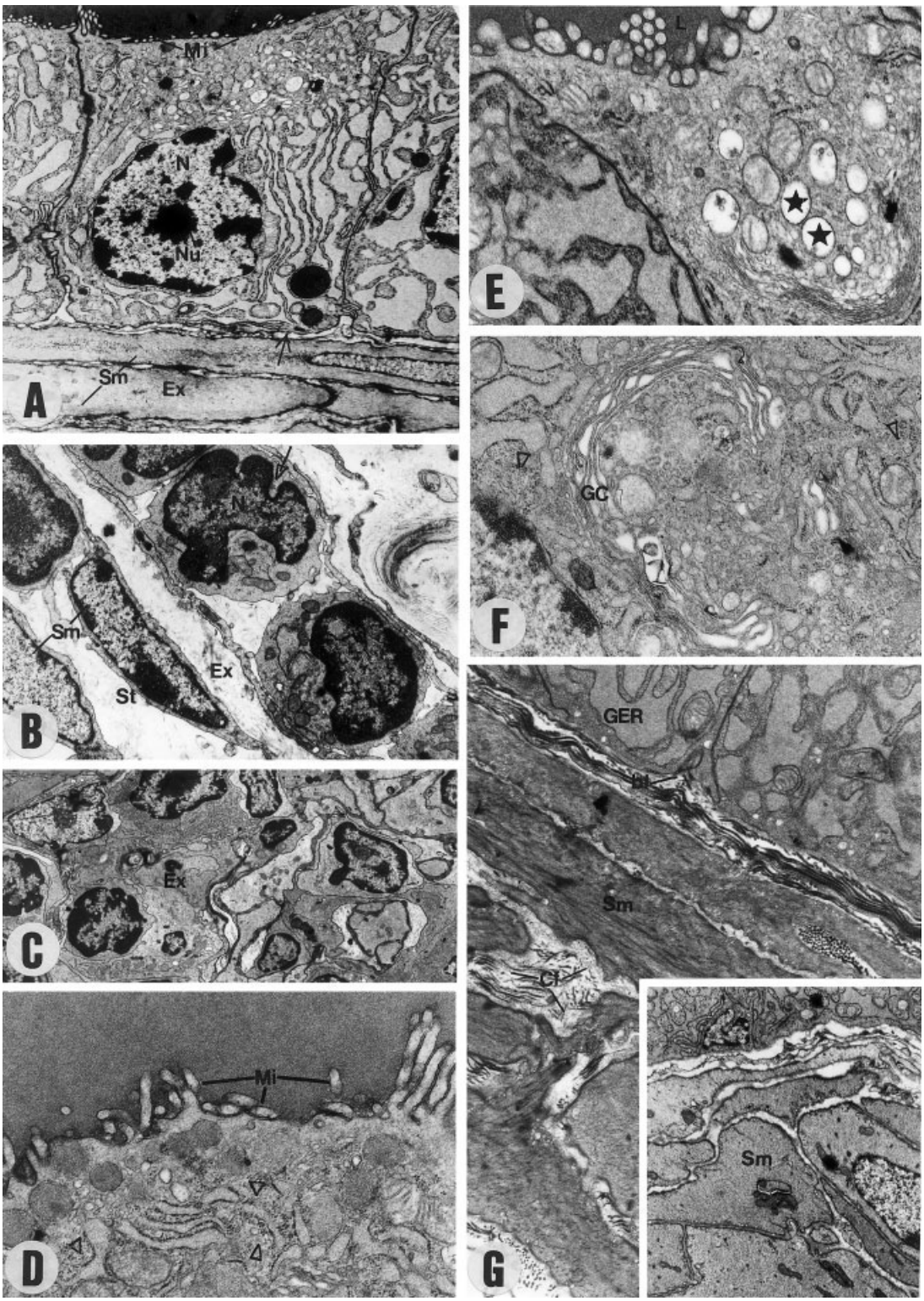

Fig. 4. Electron micrographs of the coagulating glands of AD and NOD mice. **A:** Atrophied epithelial cells. Nucleus with pleated envelope and condensed chromatin at the periphery (N). Clearly visible nucleolus (Nu). Discontinuity of microvilli covering the cell surface (Mi). Clearly visible basal lamina (arrow). Smooth muscle in the extracellular matrix (Ex). Lumen (L) ×6,120. **B:** Secretory epithelium with markedly atrophied cells. Infolded epithelial nucleus (N) with condensed chromatin and irregularities in the nuclear membrane (arrow) occupying a large part of the cytoplasm. Extracellular matrix (Ex): smooth muscle cells (Sm) with a nucleus occupying large part of the cell cytoplasm, ×6,120. **C:** Extracellular matrix (Ex): region with an inflammatory infiltrate with different cell types, ×3,672. **D:** Apical region: Cell surface presenting ruptured microvilli (Mi). Accumulation of free ribosomes (υ) ×18,000. **E:** Apical region: Apparently empty vacuoles (★). Lumen (L) ×18,000. **F:** Supranuclear region: evident dilatation of Golgi cisterns (GC). Accumulation of free ribosomes (υ) ×18,000. **G:** Basal region: involution of the cisterns of the granular endoplasmic reticulum (GER). Intact basal lamina (bl). Thickening of the extracellular matrix: smooth muscle cells (Sm), collagen fibers (Cf) ×12,000. Inset: Apparent hypertrophy of smooth muscle cells (Sm) ×3,672. A–D: NOD animals. E–H and inset: AD animals.

damental importance for the homeostasis of accessory sex glands (Grobstein, 1975; Bissell et al., 1982). Thus, interruption of this equilibrium, such as observed with androgen depletion, leads to physiological, morphological, and biochemical disorders (Okuda et al., 1991).

Several investigators have associated prostatic carcinoma and benign prostatic hypertrophy (BPH) with androgen deprivation in both men and rodents (Hawkins and Geuze, 1975; Sund et al., 1983; Isaacs and Coffey, 1989). BPH is characterized by hypertrophy of extracellular matrix components, and atrophy of the effectively secretory compartment, leading to compression of the prostatic urethra and consequently to urine retention (Berry et al., 1984). Considering the similarity of the structural changes observed in diabetic animals to those observed in castrated animals, as well as the known androgen dependence of the coagulation gland, it may be inferred that the morphological events observed in the stroma could be related to an attempt to maintain the integrity of the epithelium and, consequently, of the secretory process. In addition, the present results suggest that the deleterious effects of diabetes on the coagulation gland may be associated with the onset of diseases in this organ.

Changes in the secretory epithelium of the coagulation glands of diabetic animals were also observed. These changes mainly affected the organelles involved in the secretory process, in addition to cellular and fibrillar elements of the extracellular matrix, confirming the analyses at the light microscopy level. Drastic structural changes in the organelles involved in the secretory process have been reported to occur in the ventral lobe of the prostate of mice with streptozotocin-induced diabetes (Cagnon et al., 2000). Literature data indicate that relevant structural changes of cellular organelles occur in the accessory sex glands involved in the secretory process in castrated animals, as has been observed in experimental diabetes (Cavazos, 1975). Aumüller and Seitz (1990) also demonstrated that castration induces degradation of biological membranes in the accessory sex glands, as characterized by dilatation of Golgi cisterns and GER atrophy, leading to a faulty secretory mechanism. In addition, experiments on castrated rodents have revealed nuclei with peripheral chromatin condensation in the secretory epithelial cells of accessory sex glands, a characteristic attributed to premature occurrence of cells in different stages of programmed cell death in response to androgen depletion (Kubo et al., 1998). Thus, it may be concluded that experimental diabetes leads to important alterations in the biomembrane system of the organelles involved in the secretory process of the coagulation gland of mice, leading to a deficient secretory process and a consequent weakening of fertility. The similarities between the changes in the organelles of glandular cells observed in both diabetic and castrated animals indicate that the primary etiology of the deleterious effects of diabetic status is hormonal imbalance associated with changes in the hypothalamus-pituitary-gonadal axis. Although there was relative homogeneity in the morphological changes of the coagulation glands in both NOD and AD mice, these changes were found to be more marked in the NOD mice.

ACKNOWLEDGMENTS

The authors thank Dr. Iara Maria Silva De Luca, Sr. Norivaldo Celestino, and Sr. Marco Aurélio Ribeiro de Paula.

LITERATURE CITED

Ader M, Richey JM, Bergman RN. 1998. Evidence for direct action of aloxana to induce insulin resistence at the cellular level. Diabetologia 41:1327–1336.

Aumüller G. 1977. Lipopigment fine structure in human seminal vesicle and prostate gland epithelia. Virchows Arch B Cell Pathol 24:79–85.

Aumüller G, Seitz J. 1990. Protein secretion and secretory proccess in male accessory sex gland. Int Rev Cytol 121:127–231.

Berry SJ, Coffey DS, Walsh PC, Ewing LL. 1984. The development of human prostatic hyperplasia with age. J Urol 132:474–479.

Bissell MJ, Hall HG, Perry G. 1982. How does the extracellular matrix direct gene expression? J Theor Biol 99:31–68.

Bradshaw BS, Wolfe HG. 1977. Coagulation proteins in the seminal vesicles and coagulating gland of the mouse. Biol Reprod 16:9–36.

Cagnon VHA, Garcia PJ, Martinez FE, Martinez M, Padovani CR. 1996. Ultrastructual study of the coagulating gland of Wistar rats submitted to experimental chronic alcohol ingestion. Prostate 28: 341–346.

Cagnon VHA, Camargo AM, Rosa RM, Fabian R, Padovani CR, Martinez FE. 2000. Ultrastructural study of the ventral lobe of the prostate of mice with streptozotocin induced diabetes. Tissue Cell 32:1–9.

Carballada R, Esponda P. 1992. Role of fluid from seminal vesicles and coagulating glands in sperm transport into the uterus and fertility in rats. J Reprod Fertil 95:639–648.

Cavazos F. 1975. Fine structure and functional correlates of male accessory sex gland of rodents. Am Physiol Soc 5:353–380.

Cukierski MA, Sina JL, Pralahada J, Wise LD, Antonello JM, McDonald JS, Robertson RT. 1991. Decreased fertility in male rats administered the 5α reductase inhibitor finasteride is due to deficits in copulatory plug formation. Reprod Toxicol 5:353–362.

Daubresse JC, Meunier JC, Wilmotte J, Luyckx AS, Lefebvre PJ. 1978. Pituitary-testicular axis in diabetic men with and without sexual impotence. Diabetes Metab 4:233–237.

De Carvalho HF, Line RSP. 1996. Basement membrane associated changes in the rat ventral prostate following castration. Cell Biol Int 20:809–819.

Grobstein C. 1975. The developmental role of the intracellular matrix: a retrospective and prospective. In: Slavikin HC, Greulich RC, editors. Extracellular matrix influence on gene expression. New York: Academic Press. p 9–16.

Hawkins EW, Geuze JJ. 1975. Demonstration and partial characterization of cytosol receptors for testoterone. Biochemistry 14:3094–3101.

Hunt EL, Bailey DW. 1961. The effects of alloxan diabetes on the reproductive system of young male rats. Acta Endocrinol 38:432–440.

Isaacs JT, Coffey DS. 1989. Etiology and disease process of the benign prostatic hyperplasia. Prostate 2(suppl):33–50.

Jackson FL, Hutson JC. 1984. Altered responses to androgens in diabetic male rats. Diabetes 33:819–824.

Karnovsky JM. 1965. A formadehyde-glutaraldehyde fixative in high osmolality for use in electron microscopy. J Cell Biol 27:137a–138a.

Kiess W, Gallaher B. 1998. Hormonal control of programmed cell death/apoptosis. Eur J Endocrinol 138:482–491.

Kubo M, Uchiyama H, Ueno A, Terada N, Fujii Y, Baba T, Ohno S. 1998. Three-dimensional ultrastructure of apoptotic nuclei in rat prostate epithelial cells revealed by quick-freezing and deep-etching methods. Prostate 35:193–202.

Makino S, Kunimoto K, Muroaka Y, Mizushima Y, Katagiri K, Tochino Y. 1980. Breeding of a non obese diabetic strain of mice. Exp Anim 29:1–13.

Mariotti A, Durham J, Frederickson R, Miller R, Butcher F, Mawhinney M. 1987. Action and alterations of estradiol and retinoic acid in mouse anterior prostate gland. Biol Reprod 37:1023–1035.

Narbaitz R. 1974. Embryology, anatomy and histology of the male sex accessory glands. In: Brandes D, editor. Male sex accessory organs. New York: Academic Press. p 3–15.

Okuda Y, Fujisawa M, Matsumoto O, Kamidono S. 1991. Testosterone dependent regulation of the enzymes involved in DNA synthesis in the rat ventral prostate. J Urol 145:188–191.

Price D. 1963. Comparative aspects of development and structure in the prostate. NCI Monogr 12:1–27.

Reddy S, Londonkar R, Patil SB. 1998. Testicular changes due to graded doses of nicotine in albino mice. Ind J Physiol Pharmacol 42:276–280.

Rennie PS, Bouffard R, Bruchovsky N, Cheng H. 1984. Increased activity of plasminogen activators during involution of the rat ventral prostate. Biochem J 221:171–178.

Reynolds ES. 1963. The use of lead citrate at high pH as an electron-opaque stain in electron microscopy. J Cell Biol 17:208.

Sjöstrand NO. 1965. The adrenergic innervation of the vas deferens and the accessory male genital gland. Acta Physiol Scand 65:Suppl. 257.

Sprando RL. 1990. Perfusion of rat testis through the heart using heparin. In: Russel LD, Ettlin APS, Cleeg ED, editors. Histological and histopatological evaluation of the testis. Clearwater: Cache River Press. p 277–280.

Stefan SF. 1996. Definition and classification of diabetes including maturity-onset diabetes of the young. Diabetes mellitus: a fundamental and clinical text. p 251–295.

Sund A, Lundmo PI, Kopstad G, Tvedt K, Haugen OA. 1983. A spontaneous adenocarcinoma of the rat coagulating gland. J Steroid Biochem 19(Suppl);44s Abstr: 131.

Watson ML. 1958. Staining of tissues sections for electron microscopy with heavy metals. J Biophys Biochem Cytol 4:475.

Weibel ER, Kistler GS, Scherle WF. 1966. Practical stereological methods for morphometrics cytology. J Cell Biol 30:23–38.

Weibel ER. 1979. Stereological principles for morphometry in electron microscopic cytology. Int Rev Cytol 26:235–302.

Wichern DW, Johanson RA. 1992. Applied multivariate statistical analysis. 3rd ed. NJ: Prentice Hall. 642p.

Will JC, Vinicor F, Calle EE. 1999. Is diabetes mellitus associated with prostate incidence and survival? Epidemiology 10:313–318.

Wilson EM, French FS. 1980. Biochemical homology between rat dorsal prostate and coagulating gland. Purification of a major androgen-induced protein. J Biol Chem 255:10946–10953.